



Revista Mexicana de Física

ISSN: 0035-001X

rmf@ciencias.unam.mx

Sociedad Mexicana de Física A.C.

México

Fuentes, M.E.; Fuentes, L.; Olivera, R.; García, M.  
Meso- and nano- magnetoelectricity: a review  
Revista Mexicana de Física, vol. 53, núm. 1, enero, 2007, pp. 21-29  
Sociedad Mexicana de Física A.C.  
Distrito Federal, México

Available in: <http://www.redalyc.org/articulo.oa?id=57066107>

- How to cite
- Complete issue
- More information about this article
- Journal's homepage in redalyc.org

redalyc.org

Scientific Information System

Network of Scientific Journals from Latin America, the Caribbean, Spain and Portugal

Non-profit academic project, developed under the open access initiative

# Meso- and nano- magnetoelectricity: a review

M.E. Fuentes

*Autonomous University of Chihuahua (UACH), Campus Universitario Chihuahua, Chih. 31000, Mexico.*

L. Fuentes\*, R. Olivera, and M. Garcia

*Advanced Materials Research Center (CIMAV),*

*Complejo Industrial Chihuahua, Miguel de Cervantes 120 Chihuahua, Chih. 31109, Mexico,*

*\*e-mail: luis.fuentes@cimav.edu.mx*

Recibido el 9 de junio de 2006; aceptado el 5 de septiembre de 2006

The physics of magnetoelectric phenomena, on different scales, is discussed. At macro- and mesoscopic levels, the best performance today is obtained by magnetostrictive-piezoelectric composites. Magnetoelectric coupling is obtained by means of an elastic link. The Carman model for magneto-elasto-electric interaction is presented. Recent experimental results are commented on. A mesoscopic analysis of single-phased magnetoelectric materials is presented. Effective properties of single-crystals and textured polycrystals are mathematically characterized and references to recent experimental reports are given. Some basic questions regarding the atomic-level physics of magnetoelectric multiferroics are discussed. Quantum mechanical conditions for the co-existence of ferroelectric and ferromagnetic structures are investigated. The approach of Spaldin and coworkers, and its computational implementation, are analyzed. The search for a critical size associated with ferroic phenomena is described. Representative contributions are mentioned. Experimental work and computational modeling running at CIMAV and UACH are described.

**Keywords:** Magnetoelectricity; multiferroic materials; nano-composites.

Se discute la física de los fenómenos magnetoelectricos a diferentes escalas. A niveles macro- y mesoscópico los compósitos magnetoestrictivo-piezoelectrico exhiben hoy los mejores desempeños. El acoplamiento magnetoelectrico se obtiene mediante un vínculo elástico. Se presenta el modelo de Carman para la interacción magneto-elasto-eléctrica. Se comentan resultados experimentales representativos. Se expone un análisis mesoscópico de materiales magnetoelectricos monofásicos. Se dan referencias a desarrollos experimentales recientes. Se discuten cuestiones básicas de la física de la magnetoelectricidad a nivel atómico. Se investigan las condiciones mecano-cuánticas para la coexistencia de ferroelectricidad y ferromagnetismo. Se describe la búsqueda de un tamaño crítico para la desaparición de los efectos ferroicos. Se mencionan los trabajos experimentales y de cómputo desarrollados por CIMAV y la UACH en magnetoelectricidad.

**Descriptores:** Magnetoelectricidad; materiales multiferroicos; nanocompósitos.

PACS: 75.80.+q; 77.84.-s; 75.50.Dd

## 1. Introduction

Technological applications demand sensitive, portable, trustable and cheap magnetoelectric (ME) sensors, *i.e.*, devices that convert magnetic field variations in electric signals and vice-versa. Suggested applications include multiple-state memory devices, magnetically-modulated capacitors, electrically-excited magnetic actuators and magnetic field sensors.

There are two principal types of ME materials: magnetostrictive-piezoelectric composites and single-phase crystals and polycrystals.

Pierre Curie predicted magnetoelectricity in 1894 [1]. The first report on experimental observation of the ME effect was published by Schmid [2] in 1966. The material investigated was nickel-iodine boracite  $\text{Ni}_3\text{B}_7\text{O}_{13}\text{I}$ , a ferroelectric-ferromagnetic. In 1972 Suchetelene [3], working for the Philips Laboratories, developed the first magnetic field sensor based on ME effect. The sensitive material was a composite of  $\text{CoFeO}_4$ - $\text{BaTiO}_3$ . This initial period registered other significant papers written in Japan [4, 5], Europe [6] and the USA [7].

After some years of a relatively low level of activity, the ME effect has recently been revived, with some families of materials showing ME parameters of practical interest. Present reports refer mostly to composite materials [8–10]. A reduced number of single-phase ceramics also exhibit the desired property [11, 12].

As will be discussed below, the nanoscience boom [13] has irreversibly invaded the magnetoelectricity field. Most valuable applications of magnetoelectricity are expected from nano-multiferroic devices. The physical properties of magnetoelectric systems become much more surprising and intriguing on the nanometric scale.

The purpose of the present paper is to give a brief review of selected topics in the field of magnetoelectricity on different scales.

## 2. Magnetic coupling

### 2.1. Principal and coupling properties

We briefly summarize the meso- and macroscopic characterization of reversible thermal, elastic, electric and magnetic interactions. Both approach and notation follow the IEEE Standard on Piezoelectricity [14].

TABLE I. Thermo-elasto-electro-magnetic properties.

Property	Related magnitudes	Tensor
Heat capacity $C$	Entropy (P0) / Temperature (P0)	P0
Elasticity $s$	Strain (P2) / Stress (P2)	P4
Permittivity $\epsilon$	Displacement (P1) / Elec. Intensity (P1)	P2
Permeability $\mu$	Induction (A1) / Magn. Intensity (A1)	P2
Dilatation $\alpha$	Strain (P2) / Temperature (P0)	P2
Pyroelectricity $p$	Elec. Intensity (P1) / Temperature (P0)	P1
Pyromagnetism $i$	Induction (A1) / Temperature (P0)	A1
Piezoelectricity $g$	Elec. Intensity (P1) / Stress (P2)	P3
Piezomagnetism $b$	Induction (A1) / Stress (P2)	A3
Magnetoelectricity $m$	Elec. Intensity (P1) / Magn. Intensity (A1)	A2

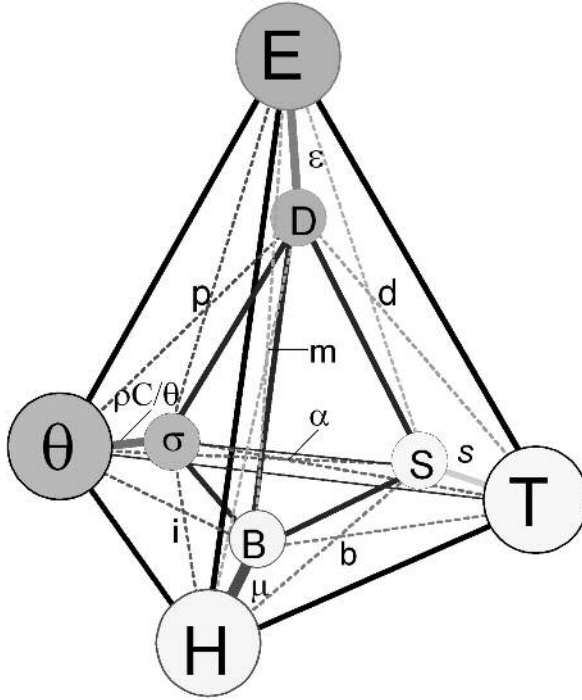


FIGURE 1. Schematic representation of constitutive relations for equilibrium properties.

Independent variables are selected according to the conditions affecting the system being considered. To fix our ideas, let us assume that the experimental setup allows us to control temperature  $\theta$ , stress  $T$ , electric field intensity  $E$ , and magnetic field intensity  $H$ . We take these quantities as independent variables. Related dependent variables are, in this case, entropy  $\sigma$ , strain  $S$ , electric displacement  $D$ , and magnetic induction  $B$ .

The behavior of a given material under the actions considered is generally described, using a linear approximation, by relations of the type  $Y = K \cdot X$ , where  $X$  (a tensor of rank  $m$ ) represents a cause and  $Y$  (tensor of rank  $n$ ), the corresponding effect. Coefficients  $K$  (rank  $m + n$ ) are *material's prop-*

*erties*, according to the definitions given in Table I. The polar (P) or axial (A) nature of representative tensors, as well as their ranks ( $0 \leq r \leq 4$ ), are included in the Table.

Heat capacity, elasticity, permittivity and permeability relate quantities of the same subsystem and therefore describe the so-called *principal* interactions. On the other hand, *coupling* properties relate magnitudes of a mixed nature. Magnetoelectricity characterizes the coupling between the electric and magnetic subsystems in a given material.

To describe the considered interactions schematically, we suggest the concentric tetrahedra in Fig. 1. “Effect” magnitudes lie in the inner spheres, and “cause” quantities in outer ones. “Cause-effect” *coupling* relations are represented by discontinuous lines.

Continuous black lines denote “cause-cause” and “effect-effect” links. Broad colored lines are associated with so-called “principal” actions, relating quantities of the same nature. Magnetoelectricity is represented by the two links  $H \rightarrow D$ ,  $E \rightarrow B$  and by the tensor  $m_{ij} = \partial D_i / \partial H_j = \partial B_j / \partial E_i$ .

A central aspect in the physics of coupling properties is given by the implications of structural symmetry on these properties. A basic idea, the Neumann’s Principle, plays a primary role regarding this question:

*Symmetry of effect is no-less than symmetry of cause.*

In materials physics, properties are “effects”, while “causes” are found in the microscopic structure (the distribution of matter, charge and electric currents).

A couple of points need to be considered in the application of Neumann’s Principle to magnetoelectricity:

- The peculiar behavior of magnetic quantities under symmetry operations.  $B$  and  $H$  fields, in the Maxwell equations, are related via cross products ( $\times$ ) with the polar vectors  $E$ ,  $J$  and the operator  $\nabla$ . Consequently, they represent cases of axial- or pseudo-vectors. They show the interesting property of remaining invariant under the inversion of coordinates. The magnetoelectric tensor  $m_{ij}$  is a second-rank axial tensor.
- A suitable symmetry concept for the investigation of

the materials' magnetic properties is that of *color-, complete- or generalized symmetry*. A color-symmetry group includes ordinary symmetry operations (denoted by the usual symmetry symbols [15]) and anti-symmetry transformations (denoted by the addition of a star \*).

Figure 2 shows the curious nature of magnetic symmetry in the simple case of a hexagonal magnetized block and its magnetic field. The physical system would be, say, a cobalt magnetic domain. Color symmetry is  $6/m\bar{2}/m^*2/m^*$ . The equatorial plane is a symmetry mirror for the magnetization current, here playing the role of a "cause". Magnetization field  $\mathbf{M}$  and magnetization current density are linked by the relationship  $\mathbf{J}_M = \nabla \times \mathbf{M}$ . Magnetic induction  $\mathbf{B}$ , the "effect", points upward. The field pattern is typical of a magnet, with North up and South down. According to Neumann's Principle, if we have a mirror plane for the current density, we must also find this symmetry for the magnetic field. Is the considered dipole field symmetric with respect to the equatorial plane? Yes, the magnetic way. This is precisely the meaning of the pseudo-vector concept.

The Neumann Principle leads to powerful analytical tools by means of the Theory of Irreducible Representations of

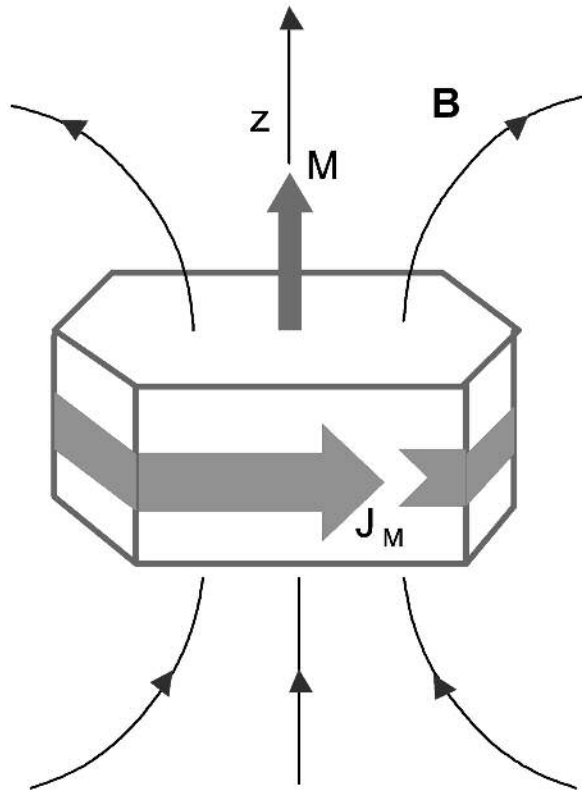


FIGURE 2. Application of Neumann's Principle to a magnetic configuration. Centrosymmetric magnetized hexagon, magnetization current distribution and magnetic field. Color-symmetry point group is  $6/m\bar{2}/m^*2/m^*$ .

TABLE II. Electric and magnetic coupling effects crystallographic point groups.

Cryst.Syst.	Point Group					PRE	PZE	PRM	PZM	ME
	Int	Sch	type							
Triclinic	1	$C_1$	e		+	+	+	+	+	+
	-1	$C_i$	c					+	+	
Monoclinic	2	$C_2$	e		+	+	+	+	+	+
	m	$C_s$	nc-ne		+	+	+	+	+	+
	2/m	$C_{2h}$	c					+	+	
Orthorhombic	222	$D_2$	e			+			+	+
	2mm	$C_{2v}$	nc-ne		+	+			+	+
	mmm	$D_{2h}$	c						+	
										+
Tetragonal	4	$C_4$	e		+	+	+	+	+	+
	-4	$S_4$	nc-ne				+	+	+	+
	4/m	$C_{4h}$	c					+	+	
	422	$D_4$	e			+			+	+
	4mm	$C_{4v}$	nc-ne		+	+			+	+
	-42m	$D_{2d}$	nc-ne			+			+	+
Trigonal	4/mmm	$D_{4h}$	c						+	
	3	$C_3$	e		+	+	+	+	+	+
	-3	$S_6$	c					+	+	
	32	$D_3$	e			+			+	+
	3m	$C_{3v}$	nc-ne		+	+			+	+
	-3m	$D_{3d}$	c						+	
Hexagonal	6	$C_6$	e		+	+	+	+	+	+
	-6	$C_{3h}$	nc-ne			+	+		+	
	6/m	$C_{6h}$	c					+	+	
	622	$D_6$	e			+			+	+
	6mm	$C_{6v}$	nc-ne		+	+			+	+
	-6m2	$D_{3h}$	nc-ne			+			+	
	6/mmm	$D_{6h}$	c						+	
Cubic	23	$T$	e			+			+	+
	m3	$T_h$	c						+	
	432	$O$	e							+
	-43m	$T_d$	nc-ne			+				
	m3m	$O_h$	c							

Legend: Int: international notation; Sch: Schoenflies notation; e: enantiomorphic; c: centric; nc-ne: non centric-non enantiomorphic. +: possible; PRE: pyroelectricity; PZE: piezoelectricity; PRM: pyromagnetism; PZM: piezomagnetism; ME: magnetoelectric effect.

Groups (*irreps*). This subject has been presented at different levels of abstraction. Some representative contributions are those given by Litvin [16–18] Djeludev [19] and Nowick [20]. A bird's eye view of the irreps' approach follows.

Consider property  $\mathbf{K}$ , which fulfills  $\mathbf{Y} = \mathbf{K} \cdot \mathbf{X}$ . To establish whether  $\mathbf{K}$  is necessarily null or not, the following procedure applies.

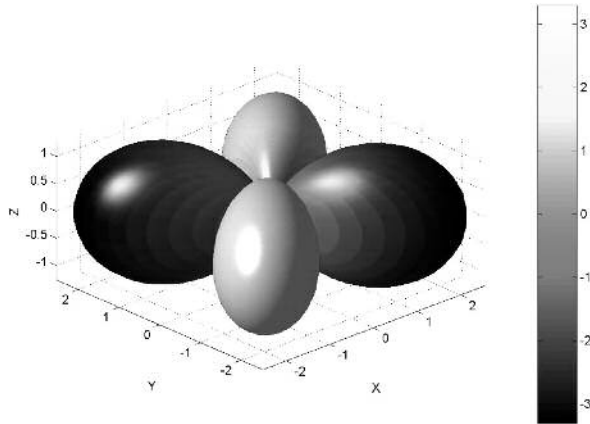


FIGURE 3. Longitudinal magnetoelectric module. Ni-Cl boracite<sup>39</sup>. Point group: mm2.

- Identify the sample's color-symmetry point group.
- Determine the characters' table and the irreps' functional bases.
- In the previous table, identify which irreps are common to  $X$  and  $Y$ , according to the tensors' characteristics.
- Clarify whether a linear relationship exists between irreps of  $X$  and  $Y$ .
- If this relationship exists, then the property considered may be present in the investigated material.

Table II resumes the possible electric and magnetic coupling effects in the 32 crystallographic point groups. In electric as well as magnetic cases, pyro-susceptible materials are

a sub-set of piezo-susceptible ones. Electric spontaneous polarization is in conflict with the inversion symmetry, but spontaneous magnetization is not.

The *Materials Physics Group* at CIMAV has prepared the software package *SAMZ* for the graphical representation of anisotropic crystal properties [21]. The so-called longitudinal modules' surfaces, derived from the properties of tensors, are plotted. Figure 3 shows the longitudinal magnetoelectric surface for a hypothetical crystal with mm2 point group. Notice positive and negative values, according to the peculiar way in which magnetic magnitudes behave under mirror symmetry.

## 2.2. Measurement of magnetoelectric response

The initial idea of measuring magnetoelectricity is simple: placing a sample in a magnetic field produces a measurable electric signal. But, parasitic signals and artifacts easily appear. Magnetoelectricity is generally weak, and electromagnetic induction in cables and sample holders is relatively strong. Several measuring systems, with different capabilities and precautions, have been reported. O'Dell [22] has published a survey of techniques. Rivera, Schmid and collaborators have published systematic improvements of ME measuring methods. Their techniques give the possibility of determining several components of the linear ME tensor [23] and also quadratic terms [24]. In an important paper [25], Rivera clarifies the definitions, units and measurement techniques of the ME effect. Present tendencies in the ME coefficients' determination include the use of dynamical meth-

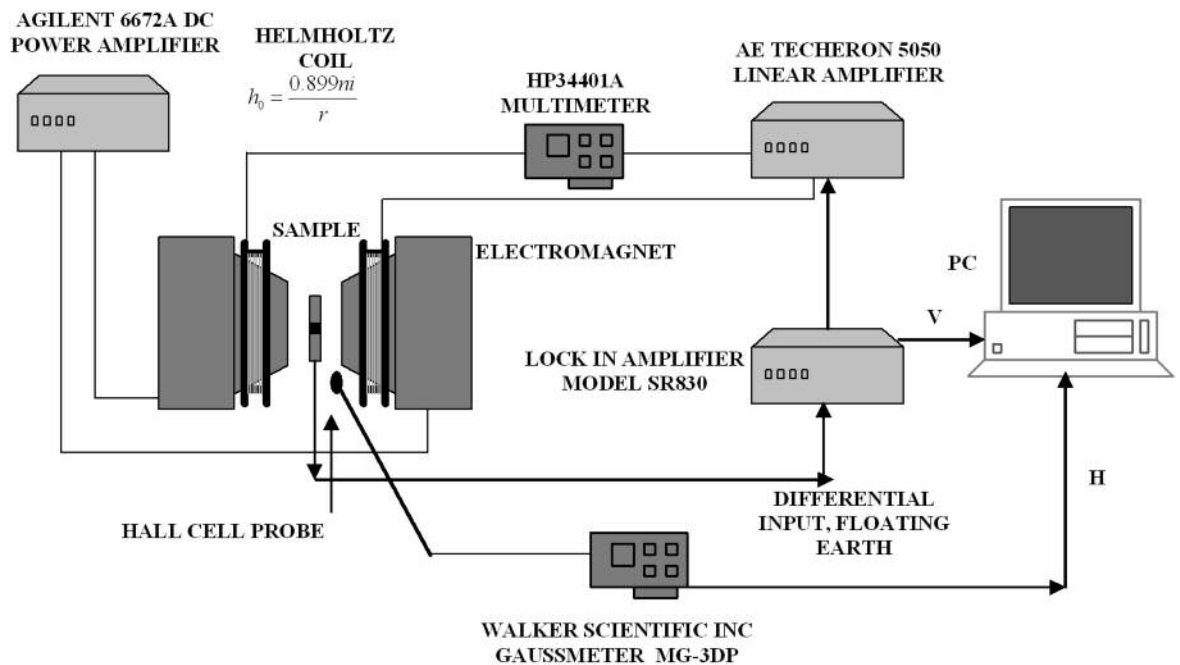


FIGURE 4. System for the dynamic measurement of ME coefficients.

TABLE III. Single-phase magnetoelectric multiferroics.

FAMILY	FORMULA	REFERENCES; COMMENTS
Perovskites	$\text{BiFeO}_3$	Rivera, Schmid [32]; $T_N = 650$ K, $T_C = 1100$ K
	$\text{BiMnO}_3$	Seshadri, Hill [33]; $T_N = 100$ K, $T_C = 450$ K
	$\text{TbMnO}_3$	Kimura <i>et al.</i> [34]; $T_N = 41$ K, $T_C = 27$ K
	$\text{HoMnO}_3$	Lorenz <i>et al.</i> [35]
	$\text{YMnO}_3$ , $\text{LaMnO}_3$	Van Acken <i>et al.</i> [36]
	$\text{BiFeO}_3$ - $\text{BaTiO}_3$ - - $\text{Bi}_{0.93}\text{La}_{0.07}\text{FeO}_3$	Mahesh, Srinivas, Kumar <i>et al.</i> [37] Sosnowska, Przenioslo <i>et al.</i> [38]
Olivines	$\text{LiCoPO}_4$	Rivera, Kornev, Gentil <i>et al.</i> [39]
	$\text{KNiPO}_4$	Lujan, Rivera [40]; $T_N = 25$ K
Boracites	$\text{Ni}_3\text{B}_7\text{O}_{13}\text{I}$	Schmid [2]
	$\text{Co}_3\text{B}_7\text{O}_{13}\text{Cl}$	Kumar, Rivera, Ye <i>et al.</i> [41]
	$\text{Cr}_3\text{B}_7\text{O}_{13}\text{Cl}$	Rivera <i>et al.</i>
Aurivillius	$\text{Bi}_5\text{Ti}_3\text{FeO}_{15}$	Ko, Bang, Shin [43]
	$\text{LaBi}_4\text{Ti}_3\text{FeO}_{15}$	James, Kumar <i>et al.</i> [44]
	$\text{Bi}_6\text{Ti}_3\text{Fe}_2\text{O}_{18}$	Srinivas, Suryanarayana <i>et al.</i> [45]
	$\text{Bi}_8\text{Ti}_3\text{Fe}_4\text{O}_{24}$	Srinivas, Kim, Hong [46]
Magnetite	$\text{Fe}_3\text{O}_4$	Chikazumi [47]
Eskolaite-Hematite	$\text{Cr}_2\text{O}_3$	Muto, Tanabe, <i>et al.</i> [48]
	$(\text{Fe}_x\text{Cr}_{1-x})_2\text{O}_3$	Popov, Belov, Vorob'ev <i>et al.</i> [49]
	$\text{Ga}_{2-x}\text{Fe}_x\text{O}_3$	Popov, Zvezdin, Kadomtseva <i>et al.</i>
Other	$\text{RMn}_2\text{O}_5$ ( $R = \text{Tm, Er, Yb, Y, Ho, Tb}$ )	Iwata, Uga, Kohn [51], Koyata, Kohn [52], Koyata, Nakamura, Iwata <i>et al.</i> [53], Ikeda, Kohn [54], Kato <i>et al.</i> [55], Saito, Kohn [56]
	$\text{Tb}_2(\text{MoO}_4)_3$ , $\text{Gd}_2(\text{MoO}_4)_3$	Wiegmann, Ponomarev <i>et al.</i> [57]
	$\text{R}_2\text{CuO}_4$ ( $R = \text{Gd, Sm, Nd}$ )	Wiegmann, Vitebski <i>et al.</i> [58]
	$\text{FeAlO}_3$	Bouree, Baudour, Elbadraoui <i>et al.</i> [59]

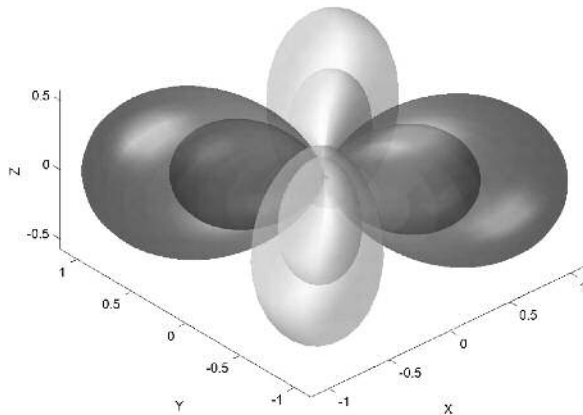


FIGURE 5. Magnetoelectric longitudinal modules for  $\text{Bi}_5\text{Ti}_3\text{FeO}_{15}$ . External surface: single crystal. Internal surface: textured polycrystal (final texture due to polarization; initial condition: sharp fiber texture) [60].

ods [26], SQUID magnetometers [27] and high-intensity pulsed magnetic fields [28]. Figure 4 is a scheme of the [AC + DC] system built at CIMAV [29], following the idea of Kumar *et al.* [26].

### 2.3. Magnetoelectric single-phase crystals and textures

ME response has been found in a relatively small number of single-phase materials. Table III shows a summary of representative findings. Some general tendencies are the following. a) as a rule, the effect is weaker than for composites, and b) observation of magnetoelectric coupling at room temperature is rare. Practically, it only occurs in  $\text{BiFeO}_3$ . Room-temperature results in other systems have not been reported with reproducibility; c) the focus today is on perovskite systems  $\text{ABO}_3$ , with  $A = \text{Bi, Y, La, Tb, Ho}$  and  $B = \text{Mn, Fe}$ ; d) bismuth-layered perovskites, so-called Aurivillius phases, also represent an interesting line of research. Work on this family is expected to grow in the coming years.

Today, one hot point in single-phase multiferroics research is related to efforts to switch the orientation of mag-

netic domains by the application of an electric field and vice-versa. The articles by Lottermorser [30] and Hur [31] represent initial achievements in this important topic.

A brief comment on crystallographic texture: crystal orientation plays an important role in magnetoelectricity (bulk matter and thin films). CIMAV software package SAMZ includes the calculation of the average properties for textured polycrystals. As an illustration, Fig. 5 represents the magnetoelectric longitudinal modules of  $\text{Bi}_5\text{Ti}_3\text{FeO}_{15}$  single-crystal and textured sample.

#### 2.4. Magnetoelectric composites

At present, as mentioned in the Introduction, the most efficient magnetoelectric transducers are based on magnetostrictive-piezoelectric composites. The magnetoelectric effect is obtained via an elastic link. In May 2005, a “Google” search in the Internet gave about 1000 reports on magnetoelectric composites. Some representative works are the following.

A number of groups in India are dedicated to this topic. Srinivas and collaborators [61] have characterized in detail the PZT- $\text{CoFe}_2\text{O}_3$  system. They have found an optimal proportion of components and proposed a “sum rule” for the prediction of the electromechanical coupling coefficient.

An international group led by G. Srinivasan (Oakland University) has given new breadth to the ferrite-PZT family. Regarding chemical composition, they have studied and optimized the influence of Zn substitution in ferrites [62]. Another work relates to the effect of electromechanical resonance in magnetostrictive-piezoelectric bilayers [63]. Optimization of sample preparation by means of hot pressing and theoretical work on coupling phenomena comprise the most recent contribution of this group [64].

Ryu *et al.* [65] have published an interesting review on ME composites. They confirm the practical advantages of composites with respect to single phase multiferroics. Ryu and coworkers establish that magnetoelectric laminate composites made with the giant magnetostrictive material, Terfenol-D, and relaxor-based piezocrystals are far superior to other contenders. The ME voltage coefficient they obtained was 5.9 V/cmOe.

Computer-aided prediction of a composite’s ME characteristics has been worked out by several authors. The works by Sabina’s groups at the National Autonomous University of Mexico (UNAM) [66] and Carman at University of California, Los Angeles (UCLA) [67] may be considered as representative. General relations for the ME coupling coefficients are given by the UCLA group [68]. An analytical solution for the case of a two-dimensional beam experiencing simultaneous field and mechanical loadings is subsequently provided. An equivalent theory is drawn for describing the ability of ferroelectro-magnets to convert and store input energy. Carman and collaborators highlight the candidacy of ferroelectro-magnets for specific applications. On the experimental side, the UCLA group has obtained a 1.2 V/cmOe magnetoelectric voltage coefficient in

a Terfenol-D/epoxy and PZT-5H [2-2] composite [69]. The coupling was achieved mechanically by bonding the piezoelectric layer between two magnetostrictive layers. The maximum in magnetoelectric voltage coefficient was measured at a frequency of 8Hz and a bias magnetic field of 103kA/m. The magnetoelectric voltage coefficient was observed to be highly dependent upon the bias magnetic field.

At present, an interesting tendency focuses on Terfenol-D/piezoelectric polymer composites. These two materials represent the most intense magnetostrictive and piezoelectric effects, respectively, known to date. According to the prediction by Nan *et al.* [70], these composites will lead to “giant” magnetoelectric phenomena. The first positive experimental results on this subject have been reported [71].

### 3. Magnetoelectricity on the nanometric scale

#### 3.1. Atomic-level understanding of multiferroic crystals

As a starting reference regarding theoretical description of ME phenomena, we mention the work by Kornev and collaborators [72]. They calculate the components of the magnetoelectric tensor for a single crystal of  $\text{LiCoPO}_4$ . The basis for the quantum mechanical model is a “one ion” approximation. Using low-order perturbation theory, variations in the g-factor due to an electric field are calculated. Theoretical results are acceptably close to experimental data.

At present, the group of N. Spaldin (UC Santa Barbara) is contributing significantly to our microscopic understanding of multiferroic events [73]. Focusing on perovskite structures, the Spaldin model for magnetoelectric multiferroics may be summarized as follows.

Two different chemical mechanisms for stabilizing the distorted structures in ferroelectric oxides are well known. Both are described as second-order Jahn-Teller effects in the literature.

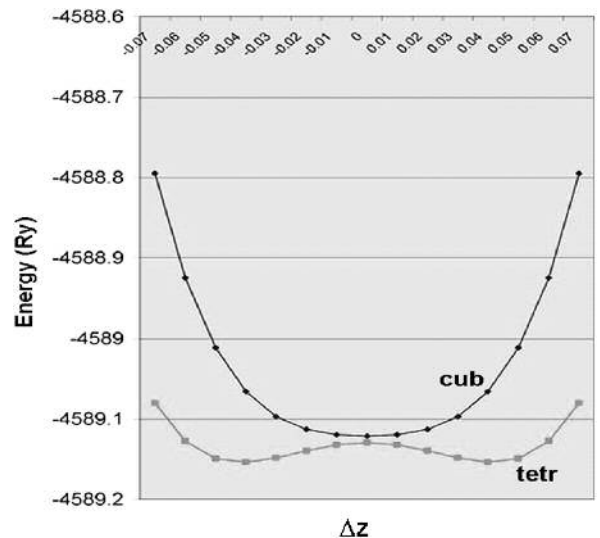


FIGURE 6 Energy as function of Ti displacement in  $\text{PbTiO}_3$ .

The first is the ligand-field hybridization of a transition metal cation by its surrounding anions. This is the origin of the off-centre displacement of the small cation in the common perovskite ferroelectrics such as  $\text{BaTiO}_3$  and  $\text{Pb}(\text{Zr,Ti})\text{O}_3$ . It was first identified theoretically in  $\text{PbTiO}_3$  and  $\text{BaTiO}_3$ , and was described as a Ti  $3d$ -O  $2p$  hybridization. An important point is that the small cation in the center of the cell ( $\text{Ti}^{4+}$ ) shows a “ $d^0$ ” condition. This favors ferroelectricity, but obviously excludes ferromagnetism. Figure 6, obtained by cooperation with the Autonomous University of Chihuahua (UACH), shows the way energy depends on  $\text{Ti}^{4+}$  off-centering for modeled cubic and tetragonal  $\text{PbTiO}_3$ . The calculations were performed by means of *ab Initio* modeling under the CASTEP program and the *generalized gradient approximation* (GGA) functional [74].

The second recognized electric polarization mechanism occurs around cations that have an  $(ns)^2$  valence electron configuration. The tendency of  $(ns)^2$  ions to lose inversion symmetry is well established, with the conventional explanation invoking a mixing between the  $(ns)^2$  ground state and a low-lying  $(ns)^1(np)^1$  excited state, which can only occur if the ionic site does not have inversion symmetry. This *stereochemical activity of the lone pair* is the driving force for off-centre distortion in Bi-based perovskites, such as  $\text{BiMnO}_3$  and  $\text{BiFeO}_3$ . Due to the presence of Mn and Fe cations, this mechanism is compatible with magnetic ordering.  $\text{BiMnO}_3$  and  $\text{BiFeO}_3$  are both ferroelectric and antiferromagnetic.

$\text{YMnO}_3$  is representative of a third ferroelectric mechanism, recently proposed by the UCSB group [75]. In this case, long-range dipole-dipole interactions and oxygen rotations both cooperate to drive the system towards the stable ferroelectric state.

Aurivillius phases, with relatively complicated crystal structures, have been theoretically characterized by Tsai *et al.* Using spin-polarized first-principle calculations, these authors conclude that  $\text{SrBi}_2\text{Ta}_2\text{O}_{11}$  forms a multiferroic film [76].

A recent paper by Spaldin and Baettig predicts that  $\text{Bi}_2\text{FeCrO}_6$  is a highly-sensitive magnetoelectric multiferroic [77].

In brief, quantum-theoretical studies of compatibility today lead the search for single-phase magnetoelectric multiferroics.

### 3.2. Multiferroic thin films

Ferroelectric and ferromagnetic thin films are well-established, active fields [78]. On the other hand, the study of simultaneous and interacting ferroelectric and ferromagnetic nanostructures is an emerging discipline. We mention some recent developments. Single-phased multiferroic thin films of  $\text{BiFeO}_3$  have been obtained and characterized by Wang and collaborators [79]. Wang reports polarization, magnetization

and coupling parameters higher than those of bulk  $\text{BiFeO}_3$ . Yun [80] finds a similar polarization, but smaller magnetization. Eerenstein [81] argues Wang's figures and states that strains do not enhance properties in the way considered by Wang.

Regarding structural characterization, a recent paper by Qi [82] reports on a high-resolution x-ray diffraction and transmission electron microscopy study of  $\text{BiFeO}_3$  thin films. Reciprocal space mapping revealed that  $\text{BiFeO}_3$  films (with a thickness of about 200 nm) were almost fully relaxed and had a rhombohedral structure. Cross-sectional, high-resolution TEM showed a thin intermediate layer of about 2 nm at the film-substrate interface. Qi's results indicate that (111)  $\text{SrTiO}_3$  substrates are adequate.

An interesting article by Son *et al.* [83] describes the process of writing polarization bits on a multiferroic  $\text{BiMnO}_3$  thin film by means of a Kelvin probe force microscope. This work opens a tangible possibility of using ME thin films for data storage.

Zheng *et al.* [84] have recently published the important achievement of self-assembled  $\text{BaTiO}_3$ - $\text{CoFe}_2\text{O}_4$  multiferroic nanocomposites. Zheng's discovery represents the beginning of a new and promising research line with several applications to nanotechnology.

A question that is on the table these days is that of the “critical size” for ferroelectricity. The generally accepted idea [85] [86] [87] is that if the crystal size is smaller than several tens of nm, the depolarizing field surrenders ferroelectric order. New experimental findings by Fong [88] and theoretical considerations by Spaldin [89] have left this criterion with a question mark. The issue today is open.

## 4. Conclusions

Magnetoelectric multiferroics define an important segment of present frontiers of knowledge. Only a limited number of single-phase materials exhibit magnetoelectricity. Recently, atomic-level reasons for this scarcity have been discovered.

Magnetostrictive-piezoelectric composites provide the best magnetoelectric systems available today. Several applications, ranging from magnetic field sensors to actuators, are being invented on the basis of these composite materials. Single-phase and composite nanometric magnetoelectrics have just been discovered. Predictably, the scientific field of nanomagnetoelectricity will experience a “boom” in the near future.

## Acknowledgements

The present research was supported by CONACYT - Project CIAM 42361.



1. P. Curie, *J. Phys.* **3** (1984) 393.
2. E. Ascher, H. Rieder, H. Schmid, and H. Stossel: *J. Appl. Phys.* **37** (1966) 1404.
3. V. Suchetelene, *Philips Res. Rep.* **27** (1972) 28.
4. K. Daido, K. Hoshikawa, and C. Uemura, *AIP (Amer. Inst. Phys.) Conf. Proc. No. 10* (Pt. 2) (1973) 1416.
5. T. Miura and E. Hirota, *Patent JP 7541095 19750415* (1975).
6. H. Schmid, *Phys. Stat. Sol.* **37** (1970) 209.
7. R.E. Newnham and D.P. Skinner, *Mater. Res. Bull.* **11** (1976) 1273.
8. J.L. Prieto, C. Aroca, E. López, M.C. Sánchez, and P. Sánchez, *IEEE Trans. on Magnetism* **34** (1998) 3913.
9. M.B. Kothale *et al.*, *Materials Chemistry and Physics* **77** (2003) 691.
10. G. Srinivasan *et al.*, *Physical Review B: Condensed Matter and Materials Physics* **64** (2001) 214408/1-214408/6.
11. F. Bouree *et al.*, *Acta Cryst. B* **52** (1996) 217.
12. S.V. Suryanarayana and A. Srinivas, *Ceramic Transactions* **106** (2000) 277.
13. N. Loder, *The Economist*, January 1<sup>st</sup> (2005).
14. *IEEE Standard on Piezoelectricity. ANSI/IEEE Std.* **176** (1987).
15. Th. Hahn (Editor), "International Tables of Crystallography". Reidel Publ. Co., Dordrech, (1983).
16. D.B. Litvin, *Acta Crystallographica A* **55** (1999) 884.
17. J. Schlessman and D.B. Litvin, *Acta Crystallographica A* **57** (2001) 114.
18. B. Shaparenko, J. Schlessman, and D.B. Litvin, *Ferroelectrics* **269** (2002) 9.
19. I.C. Djeludev, *Crystal Physics and Symmetry*, Nauka (Moscow, Russian, 2000).
20. A.S. Nowick, *Crystal Properties Via Group Theory* (Cambridge Univ. Press, Cambridge, 1995).
21. Software SAMZ. Available (free of charge) at: <http://www.cimav.edu.mx>.
22. T.H. O'Dell, *International Journal of Magnetism* **4** (1973) 239.
23. J.P. Rivera, H. Schmid, J.M. Moret, and H. Bill, *International Journal of Magnetism* **6** (1974) 211.
24. C. Tabares-Munoz, J.P. Rivera, A. Bezinges, A. Monnier, and H. Schmid, *Japanese Journal of Applied Physics* **24** (1985) 1051.
25. J.P. Rivera, *Ferroelectrics* **161** (1994) 165.
26. M.M. Kumar, A. Srinivas, S.V. Suryanarayana, G.S. Kumar, and T. Bhimasankaram, *Bulletin of Materials Science* **21** (1998) 251.
27. M. Lujan *et al.*, *Ferroelectrics* **161** (1994) 77.
28. J. Ohtani and K. Kohn, *Rikogaku Kenkyusho Hokoku, Waseda Daigaku* **102** (1982, in Japanese) 106.
29. J. Matutes-Aquino, D. Bueno-Banqués, M.E. Botello-Zubiarte, "Magnetoelectric materials" *Second Meeting of High Field Alfa Network*, INSA Toulouse (2003).
30. N. Hur *et al.*, *Nature* **429** (2004) 392.
31. T. Lottermoser *et al.*, *Nature* **430** (2004) 541.
32. H. Schmid, *Ferroelectrics* **204** (1997) 23.
33. R. Seshadri and N.A. Hill, *Chem. Mater.* **13** (2001) 2892.
34. T. Kimura *et al.*, *Nature* **426** (2003) 55.
35. B. Lorenz, "Coupling of Magnetic Order, Ferroelectricity and Lattice Strain in Multiferroic Rare Earth Manganites" ACerS 107th Congress (2005).
36. B. Van Aken, T. Palstra, A. Filippetti, and N. Spaldin, *Nature Materials* **3** (2004) 164.
37. M. Mahesh, A. Srinivas, G.S. Kumar, and S.V. Suryanarayana, *J. Phys.: Condens. Matter* **11** (1999) 8131.
38. I. Sosnowska, R. Przenioslo, P. Fischer, and V.A. Murashov, *J. Magn. Magn. Mater.* **160** (1996) 384.
39. J.P. Rivera, *J. Korean Phys. Soc.* **32** (1998) 1855.
40. M. Lujan *et al.*, *Ferroelectrics* **161** (1994) 77.
41. M. Kumar, J.P. Rivera, Z.G. Ye, S.D. Gentil, and H. Schmid, *Ferroelectrics* **204** (1997) 57.
42. J.P. Rivera, H. Schmid, J.M. Moret, and H. Bill, *International Journal of Magnetism* **6** (1974) 211.
43. T. Ko, G. Bang, and J. Shin, *Korean J. Ceram.* **4** (1998) 83.
44. A.R. James, G.S. Kumar, M. Kumar, S.V. Suryanarayana, and T. Bhimasankaram, *Mod. Phys. Lett.* **11** (1997) 633.
45. A. Srinivas, S.V. Suryanarayana, G.S. Kumar, and M.M. Kumar, *J. Phys.: Condens. Matter* **11** (1999) 3335.
46. A. Srinivas, D-W Kim, and S.V. Suryanarayana, *Mater. Res. Bull.* **39** (2004) 55.
47. S. Chikazumi, *Rigaku Denki Janaru* **28** (1997, in Japanese).
48. M. Muto, Y. Tanabe, T. Iizuka-Sakano, and E. Hanamura, *Phys. Rev. B: Condens. Matter Mater. Phys.* **57** (1998) 9586.
49. Yu. Popov *et al.*, *Zh. Eksp. Teor. Fiz.* **109** (1996, in Russian) 891.
50. Yu. Popov *et al.*, *Zh. Eksp. Teor. Fiz.* **114** (1998, in Russian) 263.
51. N. Iwata, M. Uga, and K. Kohn, *Ferroelectrics* **204** (1997) 97.
52. Y. Koyata and K. Kohn, *Ferroelectrics* **204** (1997) 115.
53. Y. Koyata, H. Nakamura, N. Iwata, A. Inomata, and K. Kohn, *J. Phys. Soc. Jpn.* **65** (1996) 1383.
54. A. Ikeda and K. Kohn, *Ferroelectrics* **169** (1995) 75.
55. S. Kato, K. Kohn, and M. Ishikawa, *Ferroelectrics* **203** (1997) 323.
56. K. Saito and K. Kohn, *J. Phys.: Condens. Matter* **7** (1995) 2855.
57. H. Wiegmann, I.M. Vitebsky, A.A. Stepanov, A.G.M. Jansen, and P. Wyder, *Key Eng. Mater.* **155** (1999) 429.
58. H. Wiegmann, I.M. Vitebsky, A.A. Stepanov, A.G.M. Jansen, and P. Wyder, *Phys. Rev. B: Condens. Matter* **55** (1997) 15304.
59. F. Bouree *et al.*, *Acta Crystallogr., Sect. B: Struct. Sci. B* **52** (1996) 217.
60. L. Fuentes, A. Rodríguez, G. Aquino de los Ríos, and A. Muñoz-Romero, *Integrated Ferroelectrics* **71** (2005) 289.

61. K. Srinivas, G. Prasad, T. Bhimasankaram and S.V. Suryanarayana, *Mod. Phys. Lett.* **14** (2000) 663.
62. G. Srinivasan, E.T. Rasmussen and R. Hayes, *Physical Review B* **67** (2003) 014418.
63. M.I. Bichurin *et al.*, *Physical Review B* **68** (2003) 132408.
64. G. Srinivasan, C.P. DeVreugd, C.S. Flattery, V.M. Laetsin, and N. Paddubnaya, *Appl. Phys. Lett.* **85** (12) (2004).
65. J. Ryu, S. Priya, K. Uchino, and H-E. Kim, *J. Electroceramics* **8** (2002) 107.
66. H. camacho-Montes, R. Rodriguez-Ramos, J. Bravo-Castillero, R. Guinovart-Diaz, and F.J. Sabina, *Integrated Ferroelectrics* **83** (2006) 49.
67. Y. Fotinich and G. Carman, *Integrated Ferroelectrics* **71** (2005) 181.
68. G. Bush and G. Carman, "Continuum Level Modeling of Linear Ferroelectro-magnetic Materials," Proceedings of the XIII International Materials Research Congress, S9-34, Cancun, Mexico (2004).
69. Nersesse Nersessian, S.W. Or, and G. Carman, "Magneto-electric Effect In Magnetostrictive/Polymer And Piezoelectric Composites". Proceedings of IMECE'03 2003 ASME International Mechanical Engineering Congress Washington, D.C., November 15–21, (2003).
70. C.W. Nan, M. Li, X. Feng, and S. Yu, *Appl. Phys. Lett* **78** (2001) 2527.
71. C-W. Nan *et al.*, *Physical Review B: Condensed Matter and Materials Physics* **71** (2005) 014102/1.
72. I. Kornev *et al.*, *Physica B* **271** (1999) 304.
73. N.A. Hill, *J. Phys. Chem. B* **104** (2000) 6694.
74. M. Ernzerhof and J.P. Perdew, *J. Chem. Phys.* **109** (1998) 3313.
75. B.B. Van Aken, T.T.M. Palstra, A. Filippetti and N.A. Spaldin, *Nature Materials* **3** (2004) 164.
76. M-H Tsai, Y-H Tang, and S.K. Dey, *J. Phys.: Condens. Matter* **15** (2003) 7901.
77. P. Baettig and N.A. Spaldin, *Applied Physics Letters* **86** (2005) 012505/1.
78. C.L. Chen *et al.*, *Appl. Phys. Lett.* **78** (2001) 652.
79. J. Wang *et al.*, *Science* **299** (2003) 1719.
80. K-Y Yun, D. Ricinshi, M. Noda, M. Okuyama, and S. Nasu, *J. of the Korean Physical Society* **46** (2005) 281.
81. W. Eerenstein *et al.*, *Science* **307** (2005) 1203.
82. X. Qi *et al.*, *Applied Physics Letters* **86** (2005) 071913/1.
83. J.Y. Son, B. Kim, C.H. Kim, and J.H. Cho, *Appl. Phys. Lett.* **84** (2004) 4971).
84. H. Zheng *et al.*, *Science* **303** (2004) 661.
85. G.B. Stephenson *et al.*, *Bull. Am. Phys. Soc.* 47 Pt. 2 (2002) 893.
86. S. Shetty, V.R. Palkar, and R. Pinto, *Pramana-J. of Phys.* **58** (2002) 1027.
87. V. Nagarayan *et al.*, *Nature Materials* **2** (2003) 43.
88. D.D. Fong *et al.*, *Science* **304** (2004) 1650.
89. N.A. Spaldin, *Science* **304** (2004) 1606.